1st Croatian Conference on Earthquake Engineering
1CroCEE
22-24 March 2021 Zagreb, Croatia

DOI: https://doi.org/10.5592/CO/1CroCEE.2021.8

# Examining the yielding displacement of concrete bridge piers equipped with shape memory alloy rebars

**Emad Abraik**
Omar Al-Mukhtar University, Derna, Libya, *eabraik@uwo.ca*

## Abstract

The common corrosion problem in conventional steel reinforcement induces a significant deterioration of the bridge pier's yielding displacement and ductility. Superelastic shape memory alloy (SE-SMA) possesses a high corrosion resistance and retrievers its original shape upon load removal. The unique material properties attract the attention for structural design use. However, the yielding displacements of members reinforced with SE-SMA materials required an investigation to fully understand the material's effect. In this paper, an extensive parametric study is performed to estimate the yielding displacement of bridge pier reinforced with SE-SMA rebars. The parametric study's size is decided by varying the reinforced concrete (RC) section characteristics, including axial load ratio, pier diameter, aspect ratio, reinforcement ratio, and confinement coefficient. Results of this study proposed an approximate formula to estimate the yielding displacement of SE-SMA bridge piers.

***Key words:*** bridge pier, shape memory alloy, yielding displacement, pushover analysis

## 1 Introduction

The corrosion resistance of conventional reinforcement steel is a major disadvantage, leading to early deterioration and stiffness degradation in reinforced concrete (RC) structures. The current focus on resiliency within structures aims to minimize the probability of damage and economic losses as well as increase the recovery function after earthquake events [1]. Following this concept, superelastic shape memory alloy (SE-SMA) attracted attention for its use as reinforcement in RC structures and bridges located in seismic and coastal zones due to its high corrosion resistance and superelasticity [2]. Several research efforts have been conducted to investigate the use of SE-SMA material in structural elements, including SMA braces [3,4], SMA-base isolation [5], and steel connection [6]. Results of these studies indicated a superior seismic performance capability compared to conventional steel material.

In concrete structures, the material was used as reinforcement in RC elements, including beam-column joints, moment frames [7], and RC shear walls [8, 9]. The results demonstrated that SE-SMA bars could effectively recover residual displacement compared to the conventional steel bars.

In parallel, numerous experimental and numerical studies have investigated the use of SE-SMA bars in bridge piers. Saiidi et al. [10] investigated the influence of utilizing SE-SMA material in bridge pier columns. Results showed that bridge piers reinforced with SE-SMA material exhibited large drift capacity combined with lower damage than the steel bridge piers. Billah and Alam [11] compared the SE-SMA bridge pier's seismic performance with different novel reinforcement materials. Results prove the superior seismic performance combined with adequate energy dissipation during the earthquake. With the same trend, Billah and Alam [12] developed performance-based damage states of SE-SMA bridge piers considering different SMA materials types. Results of their study proposed an equation to estimate the residual displacement of the considered systems. The practical demonstration of these studies was applied to a bridge in Michigan [13].

Notwithstanding all these advantages, the estimate yielding displacement of such system is missing in the literature. This paper aims to examine the approximate formula to estimate the yielding displacement for the SE-SMA bridge pier. Then, the formula is adjusted with results obtained from the numerical model to improve its accuracy.

## 2 Yielding displacement

Although SMA does not have a yielding strain, the term refers to the austenite transformation point to the martensite phase. However, Figure 1 shows the typical force-displacement relationship of the bridge pier obtained from pushover analysis. The yielding displacement ($\Delta_y$) is calculated as the secant stiffness through 75 % of the shear capacity ($V_y$), as proposed by Park [14]. The method provided an accurate estimation of the yielding displacement obtained from the conducted experimental research.

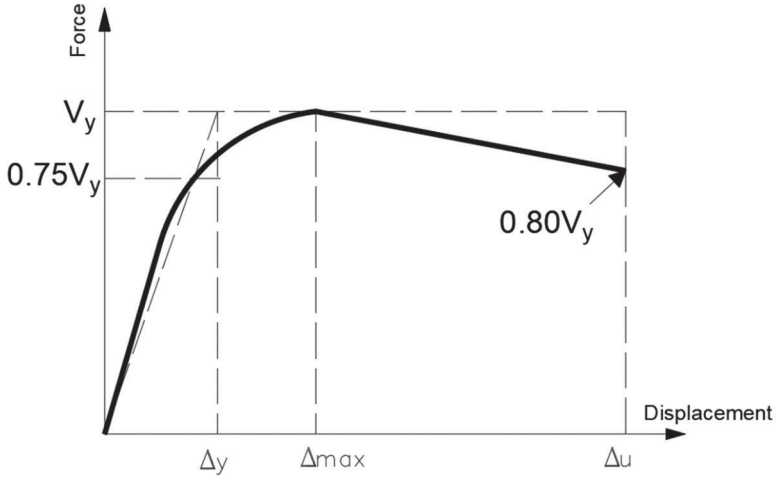


**Figure 1. Yielding displacement calculation.**

In conventional concrete bridge piers, the yielding curvature ($Ø_y$) and yielding displacement ($Δ_y$) are calculated using Eqs. (1) and (2), as proposed by Priestley et al. [15]:

$$Ø_y = 2.25\varepsilon_y / D \quad (1)$$

$$Δ_y = Ø_y H^2/3 \quad (2)$$

where $\varepsilon_y$ is the yielding strain of steel reinforcement, D is pier diameter, and H is the pier height.
In this study, the aforementioned equations were examined for SE-SMA bridge piers for rapid estimation.

## 3 Parametric study

A parametric study to examine the yielding displacement of 756 SE-SMA bridge piers are conducted using pushover analysis. These parameters are introduced in the following:

- The axial load ratio ($P/A_g f'_c$) ranges from 0.05 % to 0.35 %, P is the applied axial load, $A_g$ is the cross-section area, and $f'_c$ is the concrete compressive strength.
- Diameter (D) ranges from 400 mm to 1000 mm.
- The pier aspect ratio ranges from 6 to 10.
- The concrete confinement factor (K) of 1, 1.5, and 2.

## 4 Numerical model of SE-SMA bridge piers

The numerical model is developed in the OpenSEES software platform [16]. The bridge pier is modeled using displacement beam-column element with fiber section, as shown in Figure 2. A horizontal shear spring is added to each element using a section aggregator and is calculated using Eq. (3):

$$V = 0.4E_cA \tag{3}$$

Where $V$ is shear stiffness, $E_c$ is the concrete modulus of elasticity, and $A$ is the cross-section area.

The plastic hinge length is calculated using the recommendation by Abraik and Youssef [8], and the P-delta effect is considered in the numerical model. The conventional steel reinforcement and concrete material are modeled using steel 02 and concrete 02 material in the OpenSEES software [16], respectively.

The self-cantering material implemented in OpenSEES [16] is used to simulate the SE-SMA material located in the plastic hinge of bridge piers. Table 1 lists the input parameters used to define the self-cantering material in the OpenSEES software [16].

An experimental result conducted by Moyer and Kowalsky [17] is selected to validate the selected numerical model. The test specimen was a circular RC cantilever column with an aspect ratio of 5.33 and was subjected to a 5 % axial load ratio. Longitudinal reinforcement consisted of 12 No. 6 (19 mm diameter) grad 60 ($f_y$ = 414 MPa), providing 2.07 % longitudinal reinforcement ratio. A mechanical coupler of 120° with three rows at rebar central angles is assumed to be used to connect the SMA at the plastic hinge with steel rebar, as shown in Figure 3. The couplers showed excellent performance under repeated tensile stresses. Thus, the slippage at couplers is not considered in the numerical model.

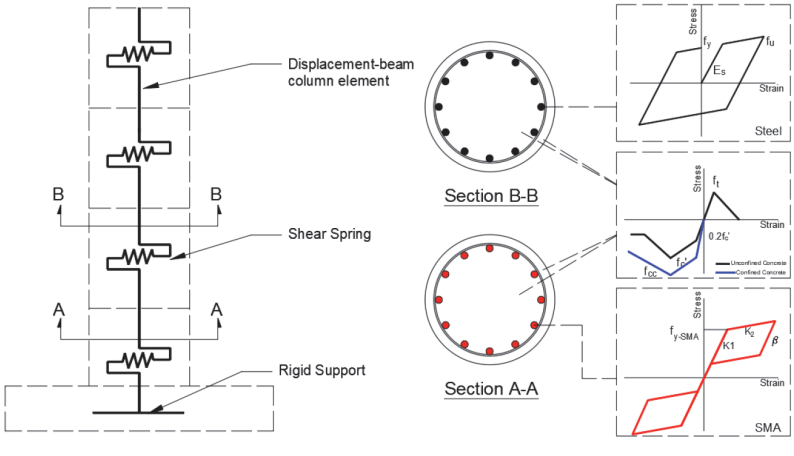


**Figure 2. Numerical model**

**Table 1. SE-SMA input parameters in the numerical model**

| Parameter | Value |
|---|---|
| $K_1$ | 36,459 MPa |
| $K_2$ | 1724 MPa |
| $F_{y\text{-}SMA}$ | 380 MPa |
| $\beta$ | 0.55 |
| Recovery strain ($\varepsilon_T$) | 7 % (mm/mm) |

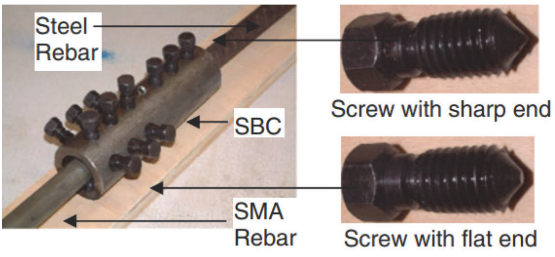


**Figure 3. Mechanical coupler connection details [18]**

As shown in Figure 4, the numerical model accurately captures the overall behavior, including peak shear capacity, ultimate displacement, and residual displacement.

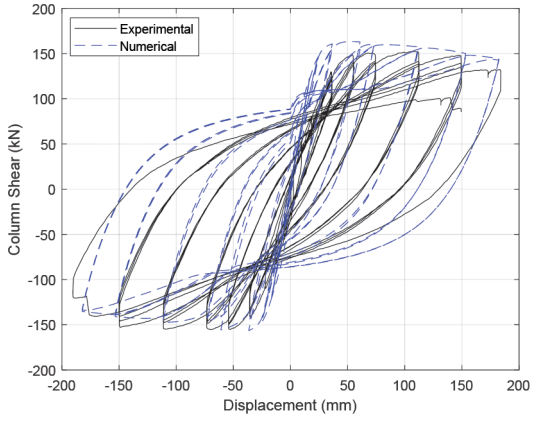


**Figure 4. Numerical validation**

## 5 Examining the approximate equation

In this section, Eq. (2) refers herein as an approximate equation examined under the aforementioned parameters. The $P/A_g f'_c$ in the practical bridge piers have a range of $0.05 \leq P/A_g f'_c \leq 0.35$. Figure 5.a shows the influence of $P/A_g f'_c$ values on the average yielding displacement ($\Delta_y$) obtained from the approximate equation, which overestimated the yielding displacement of SE-SMA bridge piers by a factor of 4.8 on average.

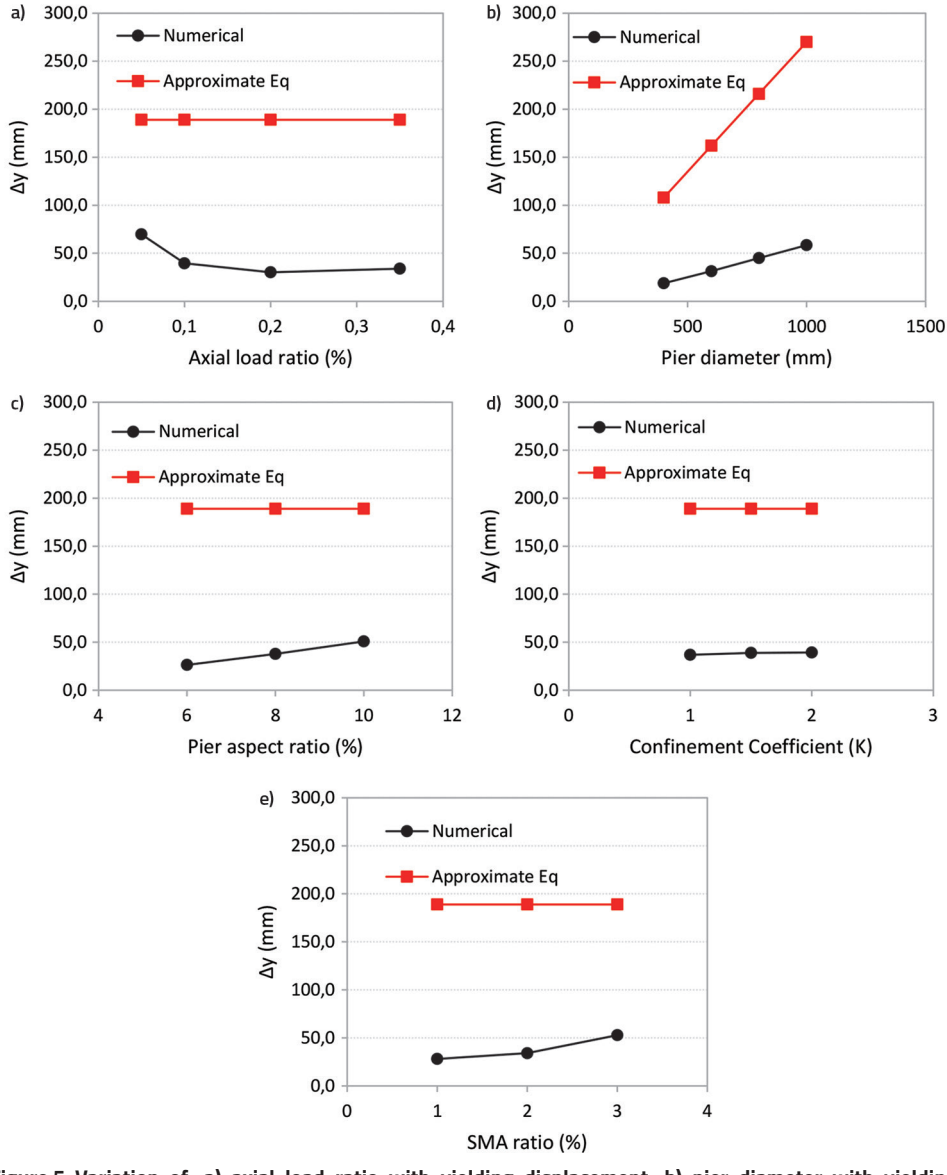


**Figure 5. Variation of: a) axial load ratio with yielding displacement; b) pier diameter with yielding displacement; c) aspect ratio with yielding displacement; d) confinement factor K with yielding displacement**

The difference appears to be constant at a higher axial load ratio (i.e., $P/A_g f'_c \geq 0.1$). Increasing the axial load ratio can delay SE-SMA bars' yielding on the tension side, explaining why the SE-SMA material exhibits a constant yielding displacement at higher axial load ratios.

Figure 5.b shows the variation of with $\Delta_y$ with the pier diameter. It is evident that increasing the pier diameter increases the $\Delta_y$. Although the approximate equation exhibits the same trend as the numerical model, the equation overestimates the $\Delta_y$ by a factor of 5.7 for low pier diameter (i.e., 400 mm) and by a factor of 4.6 for big pier diameter (i.e., 1000 mm). The source of this increase is related to the increase in pier stiffness.
Figure 5.c compares the approximate and the numerical model results. A slight increase in the is observed when the pier aspect ratio increases from 6 to 10, while the approximate equation exhibits a constant value with the pier aspect ratio variations.
The concrete confinement (K) effect on the $\Delta_y$ is illustrated in Figure 5.d. It can be observed that both the numerical and the approximate equation exhibit a constant response. It is evident that increasing the confinement effect is having a negligible impact on yielding displacement of SE-SMA bridge piers. The approximate equation also overestimates the yielding displacement by a factor of 4.8.
Eventually, Figure 5(f) plots the variation between the numerical and the approximate equation results obtained from different vertical SMA ratios. Increasing the vertical SMA ratio from 1 % to 3 % increases the by a factor of 1.9. The approximate equation provides a constant value regarding the vertical SMA ratio and the difference factor between them is between 6.7 for low steel ratio and 3.6 for high steel ratio.

## 6 Adjusted the approximate equation

Using the parametric results, two equations [i.e., Eqs. (4) and (5) refer herein as proposed equations] from statistical analysis are proposed based on axial load ratio and are expressed as follows:

$$\Delta_y = \frac{\left(0.9\varepsilon_{SMA}\right)H^2}{3D} \text{ for } P/A_g f'_c > 0.05 \tag{4}$$

$$\Delta_y = \frac{\left(0.7\varepsilon_{SMA}\right)H^2}{3D} \text{ for } P/A_g f'_c \leq 0.05 \tag{5}$$

Where $\varepsilon_{SMA}$ is the yielding of the NiTi SE-SMA material.

Figure 6 compares the results of both equations based on $P/A_g f'_c$ values. The proposed equation provides a more accurate estimation for the yielding displacement as compared to the approximate equation. These reduction factors in the proposed equation are related to the delay of SE-SMA material compared to the conventional steel reinforcement. The dispersion between both equations is increased for a higher axial load ratio, as shown in Figure 6(b).

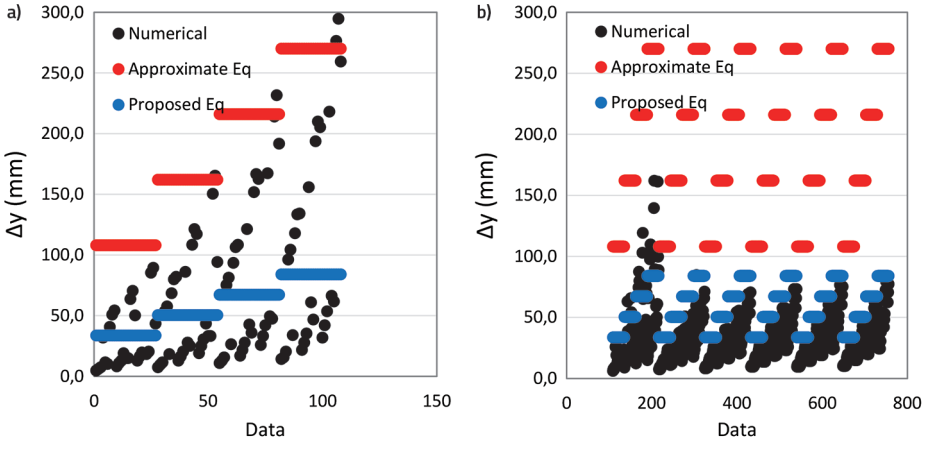


**Figure 6. Proposed equation variation with: a) axial load ratio 0.05; b) axial load ratio >0.05.**

## 7 Conclusions

This study investigates the accuracy of the approximate formula proposed by Priestley et al. [14] to estimate the yielding displacement of the circle SMA bridge pier. Then proposed equations are presented based on the performed parametric study. Several major conclusions obtained from this study are as follows:

- Axial load ratio and pier diameter significantly influence the yielding displacement of SE-SMA bridge piers compared to the influence of aspect ratio and the confinement coefficient (K). For instance, the value reduces from 70 mm to 34 mm under a high axial load ratio.
- Under different load variations, the SE-SMA material exhibited a constant response in yielding displacement when the axial load ratio ranges from 0.1 % to 0.35 %.
- The proposed equation is based on the variation of axial load ratio in order to mitigate the difference between the numerical results and the approximate equation.
- The work conducted in this paper is based on the assumption that the plastic hinge length is equal to 20 % of pier height. However, more research is needed to investigate the proposed equation's accuracy considering different plastic hinge lengths.

Eventually, several assumptions were considered in this study, including no-slippage in mechanical couplers, which are used to connect the steel reinforcement above the plastic hinge with SMA rebars in the plastic hinge. Also, shear and shear-flexural interactions are omitted from this study. Thus, future research is encouraged to address this issue.

## Acknowledgements

The author would like to express appreciation to the Civil Engineering department at Omar Al-mukhtar university, Derna.

## References


[1] Wang, B., Zhu, S., Zhao, J., Jiang, H. (2019). Earthquake resilient RC walls using shape memory alloy bars and replaceable energy dissipating devices. Smart Materials and Structures, 28(6), 065021.

[2] Billah, A.M., Alam, M.S. (2012). Seismic performance of concrete columns reinforced with hybrid shape memory alloy (SMA) and fiber reinforced polymer (FRP) bars. Construction and Building Materials, 28(1), 730-742, doi: https://doi.org/10.1016/j.conbuildmat.2011.10.020.

[3] Moradi, S., Alam, M.S., Asgarian, B. (2014). Incremental dynamic analysis of steel frames equipped with NiTi shape memory alloy braces. The Structural Design of Tall and Special Buildings, 23(18), 1406-1425.

[4] Nazarimofrad, E., Shokrgozar, A. (2019). Seismic performance of steel braced frames with self-centering buckling-restrained brace utilizing superelastic shape memory alloys. The Structural Design of Tall and Special Buildings, 28(16), e1666.

[5] Zheng, Y., Dong, Y., Li, Y. (2018). Resilience and life-cycle performance of smart bridges with shape memory alloy (SMA)-cable-based bearings. Construction and Building Materials, 158, 389-400.

[6] Fang, C., Yam, M.C., Chan, T.M., Wang, W., Yang, X., Lin, X. (2018). A study of hybrid self-centring connections equipped with shape memory alloy washers and bolts. Engineering Structures, 164, 155-168.

[7] Abraik, E. (2020). Seismic performance of shape memory alloy reinforced concrete moment frames under sequential seismic hazard. In Structures (Vol. 26, pp. 311-326). Elsevier.

[8] Abraik, E., Youssef, M.A. (2018). Seismic fragility assessment of superelastic shape memory alloy reinforced concrete shear walls. Journal of Building Engineering, 19, 142-153.

[9] Abraik, E., El-Fitiany, S.F., Youssef, M.A. (2020, October). Seismic performance of concrete core walls reinforced with shape memory alloy bars. In Structures (Vol. 27, pp. 1479-1489). Elsevier.

[10] Saiidi, M.S., O'Brien, M., Sadrossadat-Zadeh, M. (2009). Cyclic Response of Concrete Bridge Columns Using Superelastic Nitinol and Bendable Concrete. ACI Structural Journal, 106(1).

[11] Billah, A.M., Alam, M.S. (2012). Seismic performance of concrete columns reinforced with hybrid shape memory alloy (SMA) and fiber reinforced polymer (FRP) bars. Construction and Building Materials, 28(1), 730-742.

[12] Billah, A.M., Alam, M.S. (2016). Performance-based seismic design of shape memory alloy–reinforced concrete bridge piers. I: Development of performance-based damage states. Journal of Structural Engineering, 142(12), 04016140.

[13] Nehdi, M., Alam, M.S., Youssef, M.A. (2007). Development of SMA-based smart RC bridge for severe loading conditions, Actes des journées scientifiques du LCPC, 1761-1768.

[14] Park, R. (1988): Ductility evaluation from laboratory and analytical testing, In Proceedings of the 9th world conference on earthquake engineering, Tokyo-Kyoto, Japan (Vol. 8, pp. 605-616).

[15] Priestley, M., Calvi, G., Kowalsky, M. (2007) Displacement based seismic design of structures. IUSS Press: Pavia, Italy.

[16] OpenSees (2018) Open system for earthquake engineering simulation. Berkeley, CA.

[17] Moyer, M.J., Kowalsky, M.J. (2003). Influence of tension strain on buckling of reinforcement in concrete columns. ACI Structural Journal, 100(1), 75-85.

[18] Alam, M.S., Youssef, M.A., Nehdi, M.L. (2010). Exploratory investigation on mechanical anchors for connecting SMA bars to steel or FRP bars. Materials and Structures, 43(1), 91-107.